Environment-Stored Memory in Active Nematics and Extra-Cellular Matrix Remodeling

Ram M. Adar[1,*] and Jean-François Joanny[2,3,4]
[1]Department of Physics, Technion—Israel Institute of Technology, Haifa 32000, Israel
[2]Collège de France, 11 Place Marcelin Berthelot, 75005 Paris, France
[3]Laboratoire Physico-Chimie Curie, Institut Curie, Centre de Recherche, Paris Sciences et Lettres Research University, Centre National de la Recherche Scientifique, 75005 Paris, France
[4]Université Pierre et Marie Curie, Sorbonne Universités, 75248 Paris, France

(Received 14 January 2024; accepted 12 August 2024; published 13 September 2024)

Many active systems display nematic order, while interacting with their environment. In this Letter, we show theoretically how environment-stored memory acts an effective external field that aligns active nematics. The coupling to the environment leads to substantial modifications of the known phase diagram and dynamics of active nematics, including nematic order at arbitrarily low densities and arrested domain coarsening. We are motivated mainly by cells that remodel fibers in their extra-cellular matrix (ECM), while being directed by the fibers during migration. Our predictions indicate that remodeling promotes cellular and ECM alignment, and possibly limits the range of ordered ECM domains, in accordance with recent experiments.

DOI: 10.1103/PhysRevLett.133.118402

Active nematics are systems composed of self-propelling constituents capable of aligning along a shared axis with no preferred overall direction. The active isotropic-nematic transition has been studied extensively [1–4]. Similar to passive liquid crystals, order is driven by strong aligning fields, obtained by a combination of strong interactions and high densities. Unlike passive systems, activity couples order with propulsion and allows for coexistence between a dilute isotropic phase and dense nematic phase.

Active nematics are ubiquitous in biological systems at different scales. Our main motivation is cells in extra-cellular matrix (ECM), which are both capable of displaying nematic order. Growing biological evidence suggests that the interplay between cellular and ECM order is essential for tissue patterning and multicellular migration [5–9]. In particular, aligned collagen structures have been shown to greatly promote metastasis [10,11].

Cell-ECM coupling is especially evident in fibroblasts that deposit, degrade, and rearrange ECM fibers [12,13]. This has been modeled in different contexts, including wound healing [14], fibroblast alignment [15], and ECM patterning [8,16]. However, the macroscopic physical mechanisms underlying cell-environment interplay and their role in determining orientational order and dynamics are not well understood or quantified.

Our approach to understand cell-environment interplay is to consider them as a two-component active system. We recently applied such a description to explain *mechanical* feedback mechanisms between cells and ECM [17,18]. Here we focus on *chemical* remodeling. We find that environment-stored memory acts as an external field that allows for steady-state nematic order at arbitrarily low densities and constrains angular dynamics. We relate our results to recent *in vitro* experiments on fibroblasts [8,9]. While we are motivated by cells in ECM, our findings are generic and imply that the understanding of standard active matter may not apply in a dynamic environment, highlighting the need for further investigation and adaptation of existing theories.

Theory—We consider active cells and passive environment (matrix) segments in two dimensions, each described by their position and orientation, $\boldsymbol{r}$ and $\boldsymbol{n}$ for the cells and $\boldsymbol{r}'$ and $\boldsymbol{n}'$ for the matrix. Cells self-propel with a velocity $\boldsymbol{v} = v\boldsymbol{n}$ and diffuse with a diffusion coefficient D. They also align with neighboring cells and matrix segments. Matrix segments are considered to be apolar. They are enslaved to the cells that may deposit and degrade them (for more general choices, see SM in [19]). These dynamics are described by the following equations:

$$\begin{aligned}\partial_t f_{\mathrm{c}} &= -\nabla\cdot(f_{\mathrm{c}} v\boldsymbol{n}) + D\nabla^2 f_{\mathrm{c}} - k f_{\mathrm{c}} + k\rho_{\mathrm{c}} \mathrm{e}^{-E_{\mathrm{c}}}/Z_{\mathrm{c}}\\ \partial_t f_{\mathrm{m}} &= \frac{k_+}{2}\left[f_{\mathrm{c}}(\boldsymbol{r}',\boldsymbol{n}') + f_{\mathrm{c}}(\boldsymbol{r}',-\boldsymbol{n}')\right] - k_-\rho_{\mathrm{c}} f_{\mathrm{m}},\end{aligned} \tag{1}$$

where ∂_t denotes the partial time derivative. The function f_{c} (f_{m}) describes the distribution to find a cell (matrix segment) at position $\boldsymbol{r}$ ($\boldsymbol{r}'$) with orientation $\boldsymbol{n}$ ($\boldsymbol{n}'$). They are normalized such that $\int \mathrm{d}\boldsymbol{n} f_{\mathrm{c}} = \rho_{\mathrm{c}}$ is the cellular density and $\int \mathrm{d}\boldsymbol{n}' f_{\mathrm{m}} = \rho_{\mathrm{m}}$ is the matrix density.

The cellular orientation dynamics are written in terms of a tumbling rate k, and an orientation probability, given by

*Contact author: radar@technion.ac.il

the Boltzmann factor $\exp(-E_c)/Z_c$ with the effective alignment energy E_c and partition function $Z_c = \int d\boldsymbol{n} \exp(-E_c)$ [20]. This is a convenient choice that allows for the recovery of passive systems in simple limits.

Matrix deposition and degradation are described by the rates k_+ and $k_-\rho_m$ per cell, respectively. Here, we assume that cells locally deposit segments along their axis of motion and degrade segments in all orientations. Similar ingredients of cell and matrix dynamics were recently proposed as part of a two-layer Viscek model [8]. We note that Eq. (1) is written within mean field.

Averaging the different moments of the orientation angles yields mesoscopic fields that are the focus of our theory. The active cellular current density is given by $\boldsymbol{j} = v\int d\boldsymbol{n} f_c$, the cellular nematic tensor density is $\boldsymbol{Q}_c = \int d\boldsymbol{n}(\boldsymbol{nn} - \boldsymbol{I}/2) f_c$, and the matrix nematic tensor density is $\boldsymbol{Q}_m = \int d\boldsymbol{n}'(\boldsymbol{n}'\boldsymbol{n}' - \boldsymbol{I}/2) f_m$. These fields are all extensive in the number of cells or matrix segments.

We coarse-grain Eq. (1) into equations in terms of the average fields, using an approximation that neglects higher moments of f_c in $\boldsymbol{n}$ beyond the nematic tensor. In particular, we treat the orientation within mean field in terms of the interaction $E_c(\boldsymbol{n}) = -2\mathrm{Tr}[(\boldsymbol{nn} - \boldsymbol{I}/2)\boldsymbol{Q}_t]$ with the total aligning field $\boldsymbol{Q}_t = \beta_c\boldsymbol{Q}_c + \beta_m\boldsymbol{Q}_m$. It includes cell-cell and cell-matrix alignment, with the interaction strengths β_c and β_m, respectively (more general choices, including nonreciprocal interactions [21,22] are given in the SM [19]). In the absence of cell activity and cell-matrix interaction, our choice of E_c leads to an equivalent of Maier-Saupe theory [23] for compressible two-dimensional systems.

The resulting field equations are [19]

$$\begin{aligned}
\partial_t\rho_c &= D\nabla^2\rho_c - \nabla\cdot\boldsymbol{j},\\
\partial_t\boldsymbol{j} &= D\nabla^2\boldsymbol{j} - v^2\nabla\rho_c/2 - v^2\nabla\cdot\boldsymbol{Q}_c - k\boldsymbol{j},\\
\partial_t\boldsymbol{Q}_c &= D\nabla^2\boldsymbol{Q}_c - \left(\nabla\boldsymbol{j} + \nabla\boldsymbol{j}^{\mathrm{T}} - \nabla\cdot\boldsymbol{j}\boldsymbol{I}\right)/4\\
&\quad - k\boldsymbol{Q}_c + k\rho_c g(Q_t)\boldsymbol{Q}_t/Q_t,\\
\partial_t\rho_m &= \rho_c(k_+ - k_-\rho_m),\\
\partial_t\boldsymbol{Q}_m &= k_+\boldsymbol{Q}_c - k_-\rho_c\boldsymbol{Q}_m.
\end{aligned} \tag{2}$$

The first equation is the cellular continuity equation, given by the active cellular current $\boldsymbol{j}$ and passive diffusive current. The second equation is a polarization-rate equation for the active current, which we interpret below, at steady state, as a force balance equation.

The equation for $\boldsymbol{Q}_c$ includes diffusion and shear alignment (first line), as well as nonlinear alignment terms that dominate at large length scales (second line). They are written in terms of the function $g(x) = I_1(x)/I_0(x)$, where $I_n(x)$ is the modified Bessel function of the first kind [24], which results from an angular average of the Boltzmann factor $\exp(-E_c)$. The cellular dynamics include the first and second moments of the angular distribution ($\boldsymbol{j}$ and $\boldsymbol{Q}_c$, respectively), similarly to "self-propelled rods" [25–27]. Finally, the matrix dynamics are governed by cellular deposition and degradation.

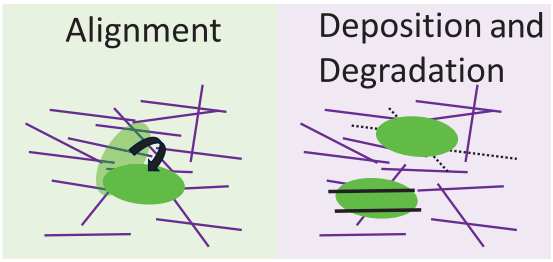

FIG. 1. Heuristic description of cell-matrix feedback. Left panel: cells (green) align with matrix segments (purple). Right panel: cells degrade existing segments (dashed black) and deposit new segments (bold black). The feedback between these processes drives the phenomena in our theory.

These equations define our framework for active nematics (cells) with environment-stored memory (matrix nematic order), which we apply for the study of ECM remodeling. Cell-matrix interplay enters the theory in two ways: cellular alignment by the matrix as part of the nematic tensor $\boldsymbol{Q}_t$ and matrix remodeling by the cells (see Fig. 1). Cellular activity enters our theory in the active current $\boldsymbol{j}$, matrix deposition and degradation, and possibly in the alignment dynamics.

Next, we focus on the consequences of remodeling on the emergence of cellular and ECM orientational order at steady state as well as typical relaxation dynamics of the cell and matrix. For brevity, we rescale times with the run time $1/k$ and lengths with the typical cellular persistence length v/k, while keeping the same notation.

Results—The standard isotropic-nematic transition in active systems is similar to a gas-liquid transition [1,28], where the alignment strength plays the role of inverse temperature. At low densities and high temperatures, the system forms a dilute isotropic gas, while at high densities and low temperatures a nematic liquid. At intermediate densities and temperatures, the two phases coexist and are generally linearly unstable. Here, we show how the matrix can break this behavior.

The key to understanding the coexistence lies in the stress. In the hydrodynamic limit of large system size and long time, the total cellular current is proportional to a divergence of a tensor that we interpret as the stress [19], $\boldsymbol{\sigma} = -[\rho_c\boldsymbol{I} + 2\boldsymbol{Q}_c/(1+2D)]$. The steady-state behavior of the cells is thus described by a constant stress tensor. We consider a possible density profile along the x direction and focus on the xx component of the stress that we denote as σ for brevity,

$$\sigma = \sigma_{xx} = -\left(\rho_c + \frac{Q_c}{1+2D}\right). \tag{3}$$

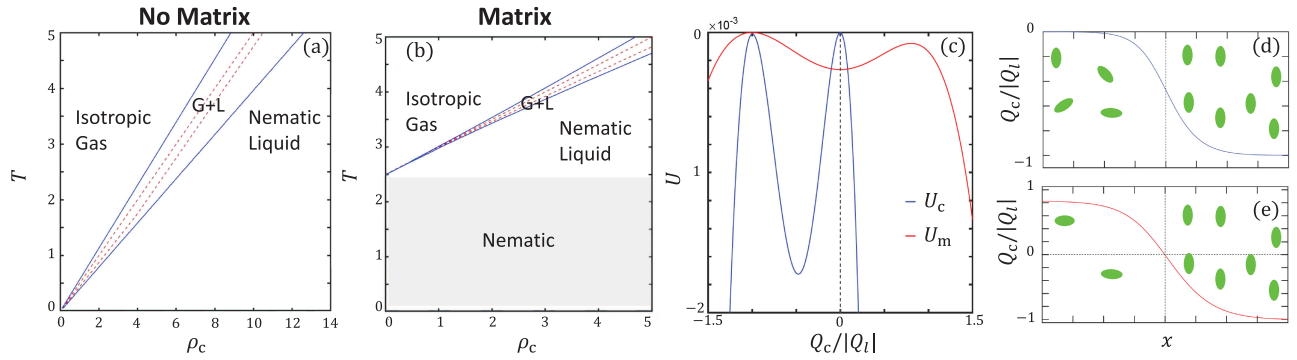

FIG. 2. (a),(b) Phase diagrams in the density and temperature plane (a) without a matrix and (b) with a matrix. We consider $\rho = \rho_c$ and $T = 1/\beta_c$. Solid blue lines are the binodal and dashed red ones are the spinodal. The values used are $D = 0.5$, $\beta_m, \rho_m = 0$ (a), and $D = 0.5$, $\beta_m = \beta_c, \rho_m = 5$ (b). (c) Comparison between cell-dominated and matrix-dominated potentials. (d),(e) Snapshots of coexistence curves from a numerical solution to the hydrodynamic equations [Eq. (2)] in the cell-dominated (d) and matrix-dominated cases (e). The green ellipses are a heuristic description of cellular orientational order. The values used are $D = 0.5$, $\sigma = -1$, and $\beta = 2.05$ (β_c in cell-dominated case and $\widetilde{\beta_m}$ in matrix-dominated case).

The first term is the ideal-gas contribution to the pressure, while the second term is an extensile active stress $\sim \boldsymbol{Q}_c$ [29]. Here, we consider ordering either along the x axis ($Q_c > 0$) or the y axis ($Q_c < 0$).

Coexistence is possible when the active stress decreases with density, compensating for the increase in ideal-gas pressure. This is the case for alignment in the y direction. The stress σ can be considered as a Lagrange multiplier that enforces the total number of cells. It is given by (minus) the density in the isotropic phase.

Next, we derive the isotropic-nematic phase diagram in the density-temperature plane, where $\beta_c, \beta_m \sim 1/T$, and the ratio β_c/β_m is kept fixed. Examples of such phase diagrams with and without a matrix (ECM) are given in Figs. 2(a) and 2(b). The region of coexistence is delimited by the binodal line (solid blue line), within which lies a region of linear instability, delimited by the spinodal line (dashed red line).

Steady-state nematic order—matrix aligns cells at arbitrarily low densities: We solve Eq. (2) at steady state. The matrix density is $\rho_m = k_+/k_-$, independent of ρ_c. The matrix nematic tensor has the same direction as the cellular one, chosen here as the x axis. We define the *intensive* nematic order of the cells and matrix, $q_c = Q_c/\rho_c$ and $q_m = Q_m/\rho_m$, and find that $q_m = q_c$ at steady state.

The matrix thus inherits the same intensive nematic order as the cells. Consequently $Q_t = (\beta_c\rho_c + \beta_m\rho_m)q_c$ at steady state, and the cellular nematic tensor solves

$$q_c = g[(\beta_c\rho_c + \beta_m\rho_m)q_c]. \tag{4}$$

This is one of our main results. By expanding the right-hand side of Eq. (4), we find that nematic order is possible for $\beta_c\rho_c + \beta_m\rho_m > 2$. The $\beta_m\rho_m$ term quantifies the matrix contribution and allows for nematic order even for vanishing cellular densities $\rho_c \approx 0$ [gray region in Fig. 2(b)]. The mechanism is simple: even dilute cells deposit a finite-density matrix after sufficiently long time. The matrix then acts as an external field that aligns the cells. Alternatively, rather than being aligned by current neighbors, cells are aligned by the memory of past neighbors, recorded by the matrix.

Next, we analyze the effect of ECM remodeling on the spinodal and binodal lines, as is plotted in Fig. 2.

Spinodal—matrix stabilizes the nematic order: The spinodal is given by $\partial\sigma/\partial\rho_c = 0$ for fixed values of β_c and β_m [19]. This threshold of linear instability is due to a negative compressibility. As the cellular density increases, the active stress overcomes the osmotic pressure and pushes cells up their concentration gradient. Note that active nematics can also be unstable due to a combination of active stress and shear alignment [30,31], but this is not the case here, where the cells are effectively extensile and align with the strain rate.

Negative compressibility occurs for $\partial Q_c/\partial\rho_c < -(1 + 2D)$ [Eq. (3)]. In the isotropic state, $Q_c \equiv 0$ and this is not possible. Deep in the ordered state, $Q_c = \pm\rho_c$, also ensuring stability. The instability is possible, therefore, only for intermediate Q_c values. For such values we expand the nonlinear terms of Eq. (4) and find its possible roots. One solution is $q_c = 0$ and the other is $q_c = -\sqrt{(\beta_m\rho_m + \beta_c\rho_c - 2)/(\beta_m\rho_m + \beta_c\rho_c)^3}$.

First, we examine the case of $\beta_m\rho_m < 2$. The cells are isotropic at low densities and become ordered at $\rho_* = (2 - \beta_m\rho_m)/\beta_c$. As $Q_c \sim \sqrt{\rho - \rho_*}$ in this case, $\partial Q_c/\partial\rho_c \ll -1$ and the system is unstable. The cell density ρ_* thus marks the gas spinodal line. Otherwise, for $\beta_m\rho_m > 2$, the slope $\partial Q_c/\partial\rho_c$ at vanishing densities is given by $\sqrt{(\beta_m\rho_m - 2)/(\beta_m\rho_m)^{3/2}} < 1$. The matrix thus increases the compressibility and ensures stability. This is why the spinodal lies outside the gray region in Fig. 2(b).

Binodal—matrix allows for coexistence between different orientations: The binodal describes, for a given temperature, the densities of the macroscopic phases at coexistence. We find it from the equation for Q_c, while replacing ρ_c by its steady-state value, $-\sigma - Q_c/(1+2D)$. Upon proper rescaling of lengths [19], we find that

$$Q_c'' = Q_c + \left(\sigma + \frac{Q_c}{1+2D}\right) g(Q_t) \equiv F(\sigma, Q_c). \quad (5)$$

This has the same structure as Newton's equation, where Q_c plays the role of position and the x coordinate the role of time, while F is the force (see also [32]). The first integral (conservation of energy) yields $E = Q_c'^2/2 + U$, where we have denoted the "potential energy" $U = -\int \mathrm{d}Q_c F(\sigma, Q_c)$.

Coexistence requires two Q_c values that have the same "potential energy" U. The coexisting phases can be either finite-sized or macroscopic, depending on the value of F. Macroscopic phases occur for $F = 0$, where it takes an infinite "time" for the Newtonian particle to switch between the phases. These two conditions set Q_l, the nematic order in the dense liquid phase, as well as $-\sigma = \rho_g$, the density in the isotropic gas phase. To summarize, we require that $Q_c = 0, Q_l$ are equally valued maxima of U at the binodal.

We highlight the effect of the environment by focusing on two limits: a cell-dominated interaction $U(\beta_m = 0) = U_c$ where there is no matrix, and a matrix-dominated one $U(\beta_c = 0) = U_m$, where the cells are aligned only by the matrix. Explicitly,

$$U_c(Q_c) = \int_0^{Q_c} \mathrm{d}Q[\rho_c(Q) g(\beta_c Q) - Q],$$
$$U_m(Q_c) = \int_0^{Q_c} \mathrm{d}Q\left[\rho_c(Q) g\left(\widetilde{\beta_m} q_c(Q)\right) - Q\right], \quad (6)$$

where $\widetilde{\beta_m} = \rho_m \beta_m$. The difference between the two cases is the magnitude of the total nematic tensor (Q_t), which appears as the argument of the nonlinear g function. In the cell-dominated case, the argument scales as the *extensive* Q_c that vanishes at small densities and the matrix-dominated cases as the *intensive* q_c. The two potentials are plotted in Fig. 2(c).

The intensive nematic order q_c in the cell-dominated case is a function of $\beta_c \rho_c$ [Eq. (4)] and both the spinodal and binodal lines are given by $\beta_c \rho_c = \text{const}$, as is displayed on Fig. 2(a). In particular, we find that the nematic order at the liquid binodal $\beta_c Q_l$ is not necessarily small [19]. Therefore, we cannot find it from an expansion of U_c, but rather from its full nonlinear form that we evaluate numerically [and see Fig. 2(c)]. We find that there is indeed a macroscopic coexistence between an isotropic gas and nematic liquid, obtained from the maxima of U_c for a specific value of ρ_g. The value ρ_l is then found by requiring a fixed stress, i.e., $\rho_g = \rho_l + Q_l/(1+2D)$. Coexistence was validated by numerical solutions of Eq. (2) in 1D [33], plotted in Fig. 2(d).

The situation is very different in the matrix-dominated case. The value of q_c in this case depends only on $\widetilde{\beta_m}$ [Eq. (4)]. We expand for small Q_c and find $U_m \sim -Q_c^2\left[Q_c^2 - 16\sigma^2 \widetilde{\beta_m}^{-3}\left(-2 + \widetilde{\beta_m}\right)\right]$. In this case, $Q_c = 0$ is a local minimum and the global maxima are $Q_c = \pm 2\sigma\sqrt{\widetilde{\beta_m}^{-3}\left(-2 + \widetilde{\beta_m}\right)}$.

Equation (4) ensures that for any solution $q_c = q$ of $F = 0$, $q_c = -q$ is also a solution. It can be shown analytically [19] that $q_c < 0$ is the global maximum, while $q_c > 0$ is a local one, as demonstrated by a numerical plot of U_m in Fig. 2(c). This form of U_m allows for coexistence between finite domains with nematic order in the x and y directions. For example, a nematic order $q_c = q > 0$, forced by surface anchoring, will transition to $q_c = -q$ in the bulk, along a thickness that diverges logarithmically with $\widetilde{\beta_m} - 2$ [19].

The coexistence between differently oriented domains is verified by numerical solutions of Eq. (2) in 1D [33], plotted in Fig. 2(e). This new type of coexistence is possible because cells order at arbitrarily low densities. Then, cells aligned along the x direction at very low densities can exert a positive active stress that matches σ. The exact form of coexistence profiles depends on angular dynamics, as explained next.

Angular dynamics—matrix possibly arrests domain coarsening: Finally, we focus on angular dynamics. While the system is invariant under global rotations of the cells and matrix together, their preferred mutual alignment results in a finite relaxation rate of their relative angle that is independent of system size. We define the angle between the preferred axis of the cells and the x axis as ϕ_c such that the two independent terms in $\boldsymbol{Q}_c$ are $Q_c \cos(2\phi_c)/2$ and $Q_c \sin(2\phi_c)/2$. We similarly define ϕ_m for the matrix. The relative angle between them is $\alpha/2 = \phi_c - \phi_m$. We rewrite Eq. (2) in terms of Q_c, Q_m, ϕ_c, and ϕ_m, and find that [19]

$$\partial_t \alpha = -\left[k\beta_m \rho_m \frac{q_m}{q_c}\frac{g(Q_t)}{Q_t} + k_+ \frac{\rho_c}{\rho_m}\frac{q_c}{q_m}\right] \sin\alpha, \quad (7)$$

where we have included the timescale $1/k$ explicitly. Note that all the densities and nematic orders also evolve in time and are coupled with α, e.g., via shear alignment.

The two terms in the parenthesis on the right-hand side of Eq. (7) describe the dynamics of the cells and matrix, respectively. In the ordered state, their characteristic rates scale as $k\beta_m\rho_m/(\beta_m\rho_m + \beta_c\rho_c)$ and $k_-\rho_c$, respectively [19]. The cellular rate depends on the typical cellular reorientation rate and the strength of its alignment to the matrix field, while the matrix rate is defined by the degradation rate. The interplay between these two rates determines whether the cells are free to rotate with the matrix constantly

remodeling according to the cells $[k_-\rho_c \gg k\beta_m\rho_m/(\beta_m\rho_m+\beta_c\rho_c)]$ or the cells are pinned to the matrix $[k_-\rho_c \ll k\beta_m\rho_m/(\beta_m\rho_m+\beta_c\rho_c)]$.

The latter implies that suppression of cellular relaxation dynamics. For example, consider ordered cellular domains of typical size l with different orientations (different ϕ_c values), such as alternating bands of width l. As long as $k\beta_m\rho_m/(\beta_m\rho_m+\beta_c\rho_c) \gg D_t/l^2$, $k_-\rho_c$, we expect these domains to remain frozen rather than relax into a common orientation, as is the usual case (see Supplemental Material figure in [19]). Here, we have denoted D_t as the total translational diffusion coefficient. In our model, it is given by $D_t = D + v^2/(4k)$.

Discussion—This work demonstrates how environment-stored memory qualitatively changes the known behavior of active nematics. The underlying mechanism is generic: active particles generate a finite external field even for vanishing densities. Our findings open an avenue for novel behavior of active systems. Arrested domain coarsening, for example, suggests that the steady state may contain a signature of the initial conditions. Environment-induced relaxation dynamics should also slow down defect dynamics (as was shown very recently in [34]) and possibly arrest typical instabilities, such as nematic bands at coexistence [1] and flow transitions [30]. Finally, this may also decrease the role of fluctuations beyond mean field.

Our finding are useful in understanding ECM remodeling by cells and its consequences on cellular and tissue dynamics. We focus on quasi-2D, *in vitro* studies of fibroblasts and their derived matrices (see, e.g., Ref. [9]). The cells exchange momentum with the underlying substrate, as is the case in "dry" active systems. The rigid substrate also suppresses elastic matrix deformations. Nevertheless, ECM displays orientational order for cellular densities of the order 10^{-4} μm^{-2}, which correspond to $\rho_c \approx 10^{-2}$, as can be explained by the memory effect in our theory (see also [15]). While matrix elasticity is considerably more important in 3D systems, it may still play some role in 2D and is expected to serve as another mechanism for alignment [35,36]. Generally, ECM rheology is complex, including visco-plastic contributions [37].

It was recently reported [8] that fibroblast-ECM interaction promotes alignment in nonaligned ECMs, but may also decrease the range of alignment. This is explained by our theory in a simple way: increasing the interaction means a larger cellular aligning field Q_t, leading to alignment. At the same time, increasing β_m also increases the rate of cellular relaxation to the matrix, and may thus suppress domain coarsening. For dilute cells, the degradation rate $k_-\rho_c$ is negligible, and the memory effect of the matrix persists for long times. Assuming that the translational diffusion is mainly active ($D_t \sim v^2/k$), we predict a domain size of the order of the cellular persistence length, i.e., of the order 10 μm. This is consistent with experimental findings [8,9]. In a future work, we will further apply our framework to predict ECM patterns observed in vivo.

In conclusion, our work demonstrates the profound effect of environment-stored memory on the steady state and dynamics of active nematics, especially in the biological context of ECM remodeling. It is generic in nature and is expected to play a similar role in additional active systems, including polar and synthetic.

Acknowledgments—We thank Erik Sahai and Raphaël Voituriez for useful discussions.

[1] H. Chaté, Dry aligning dilute active matter, Annu. Rev. Condens. Matter Phys. **11**, 189 (2020).
[2] A. Peshkov, I. S. Aranson, E. Bertin, H. Chaté, and F. Ginelli, Nonlinear field equations for aligning self-propelled rods, Phys. Rev. Lett. **109**, 268701 (2012).
[3] S. Ngo, A. Peshkov, I. S. Aranson, E. Bertin, F. Ginelli, and H. Chaté, Large-scale chaos and fluctuations in active nematics, Phys. Rev. Lett. **113**, 038302 (2014).
[4] R. Großmann, F. Peruani, and M. Bär, Mesoscale pattern formation of self-propelled rods with velocity reversal, Phys. Rev. E **94**, 050602(R) (2016).
[5] A. G. Clark and D. M. Vignjevic, Modes of cancer cell invasion and the role of the microenvironment, Curr. Opin. Cell Biol. **36**, 13 (2015).
[6] J. Alexander and E. Cukierman, Stromal dynamic reciprocity in cancer: Intricacies of fibroblastic-ecm interactions, Curr. Opin. Cell Biol. **42**, 80 (2016).
[7] S. V. Helvert, C. Storm, and P. Friedl, Mechanoreciprocity in cell migration, Nat. Cell Biol. **20**, 8 (2018).
[8] E. Wershof, D. Park, R. P. Jenkins, D. J. Barry, E. Sahai, and P. A. Bates, Matrix feedback enables diverse higher-order patterning of the extracellular matrix, PLoS Comput. Biol. **15**, e1007251 (2019).
[9] D. Park, E. Wershof, S. Boeing, A. Labernadie, R. P. Jenkins, S. George, X. Trepat, P. A. Bates, and E. Sahai, Extracellular matrix anisotropy is determined by TFAP2C-dependent regulation of cell collisions, Nat. Mater. **19**, 227 (2020).
[10] M. W. Conklin, J. C. Eickhoff, K. M. Riching, C. A. Pehlke, K. W. Eliceiri, P. P. Provenzano, A. Friedl, and P. J. Keely, Aligned collagen is a prognostic signature for survival in human breast carcinoma, Am. J. Pathol. **178**, 1221 (2011).
[11] K. S. Kopanska, Y. Alcheikh, R. Staneva, D. Vignjevic, and T. Betz, Tensile forces originating from cancer spheroids facilitate tumor invasion, PLoS One **11**, e0156442 (2016).
[12] R. Phillips, J. Kondev, J. Theriot *et al.*, *Physical Biology of the Cell* (Garland Science, 2009).
[13] F. Grinnell, Fibroblast biology in three-dimensional collagen matrices, Trends Cell Biol. **13**, 264 (2003).
[14] L. Olsen, P. K. Mainia, J. A. Sherratt', and B. Marchant, Simple modelling of extracellular matrix alignment in dermal wound healing I. Cell flux induced alignment, Comput. Math. Methods Med. **1**, 175 (1998).
[15] X. Li, R. Balagam, T.-F. He, P. P. Lee, O. A. Igoshin, and H. Levine, On the mechanism of long-range orientational order

of fibroblasts, Proc. Natl. Acad. Sci. U.S.A. **114**, 8974 (2017).
[16] J. C. Dallon, J. A. Sherratt, and P. K. Maini, Mathematical modelling of extracellular matrix dynamics using discrete cells: Fiber orientation and tissue regeneration, J. Theor. Biol. **199**, 449 (1999).
[17] R. M. Adar and J. F. Joanny, Permeation instabilities in active polar gels, Phys. Rev. Lett. **127**, 188001 (2021).
[18] R. M. Adar and J.-F. Joanny, Active-gel theory for multicellular migration of polar cells in the extra-cellular matrix, New J. Phys. **24**, 073001 (2022).
[19] See Supplemental Material at http://link.aps.org/supplemental/10.1103/PhysRevLett.133.118402 for the derivation of Eqs. (2)–(7) and the details of the calculations presented in the Letter.
[20] As cells are deformable and interact among themselves and with ECM via adhesion bonds, we describe the alignment via an interaction, E_c. Generally, alignment can also be driven by excluded volume between hard rods.
[21] Z. You, A. Baskaran, and M. C. Marchetti, Nonreciprocity as a generic route to traveling states, Proc. Natl. Acad. Sci. U.S.A. **117**, 19767 (2020).
[22] M. Fruchart, R. Hanai, P. B. Littlewood, and V. Vitelli, Nonreciprocal phase transitions, Nature (London) **592**, 363 (2021).
[23] P.-G. De Gennes and J. Prost, *The Physics of Liquid Crystals* (Oxford University Press, New York, 1993), 83.
[24] M. Abramowitz, I. A. Stegun, and R. H. Romer, *Handbook of Mathematical Functions with Formulas, Graphs, and Mathematical Tables* (American Association of Physics Teachers, 1988).
[25] M. C. Marchetti, J. F. Joanny, S. Ramaswamy, T. B. Liverpool, J. Prost, M. Rao, and R. A. Simha, Hydrodynamics of soft active matter, Rev. Mod. Phys. **85**, 1143 (2013).
[26] F. Peruani, A. Deutsch, and M. Bär, Nonequilibrium clustering of self-propelled rods, Phys. Rev. E **74**, 030904(R) (2006).
[27] A. Baskaran and M. C. Marchetti, Enhanced diffusion and ordering of self-propelled rods, Phys. Rev. Lett. **101**, 268101 (2008).
[28] A. P. Solon and J. Tailleur, Revisiting the flocking transition using active spins, Phys. Rev. Lett. **111**, 078101 (2013).
[29] While our theory corresponds to an extensile active stress, cells such as fibroblasts are often contractile. The same qualitative results apply in the contractile case. The main difference is that the nematic order will form along the x direction, rather than the y direction.
[30] R. Voituriez, J.-F. Joanny, and J. Prost, Spontaneous flow transition in active polar gels, Europhys. Lett. **70**, 404 (2005).
[31] G. Duclos, C. Blanch-Mercader, V. Yashunsky, G. Salbreux, J. F. Joanny, J. Prost, and P. Silberzan, Spontaneous shear flow in confined cellular nematics, Nat. Phys. **14**, 728 (2018).
[32] A. P. Solon, J.-B. Caussin, D. Bartolo, H. Chaté, and J. Tailleur, Pattern formation in flocking models: A hydrodynamic description, Phys. Rev. E **92**, 062111 (2015).
[33] Equation (2) was solved numerically in 1D using the "pdepe" function in MATLAB with zero-flux boundary conditions. As an initial condition, we consider a homogeneous cellular density ρ_c with $j, Q_c = 0$ and no matrix segments ($\rho_m, Q_m = 0$), which are supplemented by small normally distributed fluctuations in ρ_c, j, and Q_c.
[34] C. Jacques, J. Ackermann, S. Bell, C. Hallopeau, C. Perez-Gonzalez, L. B, X. Trepat, B. Ladoux, A. Maitra, R. Voituriez *et al.*, Aging and freezing of active nematic dynamics of cancer-associated fibroblasts by fibronectin matrix remodeling, bioRxiv (2023).
[35] R. De, A. Zemel, and S. A. Safran, Dynamics of cell orientation, Nat. Phys. **3**, 655 (2007).
[36] A. Livne, E. Bouchbinder, and B. Geiger, Cell reorientation under cyclic stretching, Biophys. J. **106**, 42a (2014).
[37] A. Elosegui-Artola, The extracellular matrix viscoelasticity as a regulator of cell and tissue dynamics, Curr. Opin. Cell Biol. **72**, 10 (2021).